Published in final edited form as:
Free Radic Biol Med. 2007 April 15; 42(8): 1193–1200.

Mn PORPHYRIN-BASED SOD MIMIC, MnTE-2-PyP^{5+}, TARGETS MOUSE HEART MITOCHONDRIA

Ivan Spasojevic[1,*], **Yumin Chen**[2], **Teresa J. Noel**[2], **Yiqun Yu**[1], **Marsha P. Cole**[2], **Lichun Zhang**[1], **Yunfeng Zhao**[2], **Daret K. St Clair**[2], and **Ines Batinic-Haberle**[3,*]

1 *Department of Medicine, Duke University Medical Center, Durham, NC 27710*

3 *Department of Radiation Oncology, Duke University Medical Center, Durham, NC 27710*

2 *Graduate Center for Toxicology, University of Kentucky, Lexington, KY, 40536*

Abstract

The Mn(III) *meso*-tetrakis(*N*-ethylpyridinium-2-yl)porphyrin, Mn^{III}TE-2-PyP^{5+} (AEOL-10113) has proven effective in treating oxidative stress-induced conditions including cancer, radiation damage, diabetes, and central nervous system trauma. *The ortho cationic pyridyl nitrogens of MnTE-2-PyP^{5+} are essential for its high antioxidant potency.* The exceptional ability of Mn^{III}TE-2-PyP^{5+} to dismute $O_2^{\cdot -}$ parallels its ability to reduce $ONOO^-$ and $CO_3^{\cdot -}$. Decreasing levels of all these reactive species is considered its predominant mode of action, that may also involve redox-regulation of signaling pathways. Recently, Ferrer-Sueta *at al* (*Free Radic. Biol Med*. 2006) showed, with submitochondrial particles, that ≥ 3 μM Mn^{III}TE-2-PyP^{5+} was able to protect components of the mitochondrial electron transport chain from peroxynitrite-mediated damage. Our study complements their data in showing, for the first time that μM mitochondrial concentrations of Mn^{III}TE-2-PyP^{5+} are obtainable *in vivo*. For this study we have developed a new and sensitive method for Mn^{III}TE-2-PyP^{5+} determination in tissues. The method is based on the exchange of porphyrin Mn^{2+} with Zn^{2+}, followed by the HPLC/fluorescence detection of Zn^{II}TE-2-PyP^{4+}. At 4 and 7 hours after a single 10 mg/kg intraperitoneal administration of Mn^{III}TE-2-PyP^{5+}, the mice (8 in total) were anesthesized and perfused with saline. Mitochondria were then isolated by the method of Mela and Seitz (*Methods Enzymol.* 1979). We found Mn^{III}TE-2-PyP^{5+} localized in heart mitochondria to 2.95 ng/mg protein. Given the average value of 0.6 μL/mg protein, the calculated Mn^{III}TE-2-PyP^{5+} concentration is 5.1 μM, which is sufficient to protect mitochondria from oxidative damage.

This study establishes for the first time, that Mn^{III}TE-2-PyP^{5+}, a highly-charged metalloporphyrin, is capable of entering mitochondria in vivo at levels sufficient to exert there its antioxidant action; such a result encourages its development as a prospective therapeutic agent.

*Corresponding authors: Ivan Spasojevic, Department of Medicine, Duke University Medical Center, Durham, NC 27710, Tel: 684-8311, Fax: 684-9094, e-mail: spaso001@mc.duke.edu, Ines Batinic-Haberle, Department of Radiation Oncology, Duke University Medical Center, 231 Nanaline H. Duke, Box 3711, Durham, NC 27710, Tel: 919-684-2101, Fax: 919-684-8885, e-mail: ibatinic@duke.edu
Present addresses: *Marsha P. Cole*: Department of Medicine-Pharmacology, University of Pittsburg, BSTWR E1314 Pittsburgh, PA 15260
Yunfeng Zhao, Department of Pharmacology, Toxicology & Neuroscience, Louisiana State University Health Science Center, Shreveport, LA 71130

Keywords

Mn^{III}TE-2-PyP^{5+}; AEOL-10113; SOD mimic targeting mitochondria; HPLC/fluorescence detection of Mn porphyrin *in vivo*; heart mitochondria; Mn porphyrin/Zn porphyrin exchange

Introduction

Due to the key role of mitochondria in health and diseases, compounds able to enter the mitochondria were actively sought [1–4]. Murphy's group has been developing mitochondria-targeted ubiquinones [1,2]. These compounds have a lipophilic triphenylphosphonium cation attached to coenzyme Q by the way of an alkyl linker. Kalyanaraman's group showed that carboxyproxyl nitroxide linked to triphenylphosphonium ion can inhibit peroxide-induced oxidative damage and apoptosis [3]. More recently Asayama et al [4] prepared a Mn^{III}TM-4-PyP^{5+} derivatized with mitochondrial targetting peptide.

Since it was designed [5], MnTE-2-PyP^{5+} has been extensively studied *in vitro* [5–18], and successfully utilized in animal models of different diseases [19–29]. Its high efficacy arises from its favorable, biologically compatible metal-centered redox potential ($E_{1/2}$ = +228 mV *vs* NHE). Such a potential, which is similar to the potential of superoxide dismutases, allows it to perform both steps of the catalysis of O_2^- dismutation at nearly identical, high rates [8]. This positive potential is predominantly due to the presence of the positively charged *ortho* pyridyl nitrogens that exert a strong electron-withdrawing effect upon the Mn. In addition, the *ortho* positive charges (forming a funnel) provide electrostatic facilitation for the reaction of MnTE-2-PyP^{5+} with negatively charged reactive species such as O_2^-, $ONOO^-$ and CO_3^- [11]. We have shown that a monocationic parent Mn(III) porphyrin, $Mn^{III}Br_8$T-2-PyP^+, possessing identical $E_{1/2}$ as Mn^{III}TE-2-PyP^{5+}, is more than 100-fold less potent a catalyst of O_2^- dismutation [11]. The ability of MnTE-2-PyP^{5+} to dismute O_2^- parallels its ability to scavenge $ONOO^-$ and CO_3^- [10,15]. As a consequence of highly positive $E_{1/2}$ for Mn^{III}P/Mn^{II}P redox couple, Mn^{III}TE-2-PyP^{5+} is easily reducible by low-molecular weight cellular reductants such as ascorbic acid, tetrahydrobiopterin and glutathione [5]. Thus scavenging of reactive species by Mn^{III}TE-2-PyP^{5+} is likely to be coupled to cellular reductants.

Although essential for its action, the multiply cationic nature of MnTE-2-PyP^{5+} may decrease its distribution within the cell and its organelles. Recently, Ferrer-Sueta et al have elegantly shown with submitochondrial particles that ≥ 3 μM Mn^{III}TE-2-PyP^{5+} is preferable to other Mn (III) porphyrins such as Mn^{III}TM-4-PyP^{5+} and $Mn^{III}TBAP^{3-}$, due to its easy reducibility by Complex I and Complex II of the mitochondrial electron transport chain, as well as by flavoenzymes such as xanthine oxidase and glucose oxidase [14]. The reduced porphyrin, Mn^{II}TE-2-PyP^{4+} in turn effectively reduces peroxynitrite, superoxide and carbonate radical [14]. The catalytic cycle of Mn^{III}TE-2-PyP^{5+} protects not only Complex II but also other components of the mitochondrial electron transport chain [14]. Our study was intended to complement the work of Ferrer-Sueta *et al* [14] by showing that mitochondrial micromolar levels of Mn^{III}TE-2-PyP^{5+} are attainable *in vivo*. Such a finding justifies further optimization of these compounds as potential therapeutics.

Thus far no sensitive method for the *in vivo* detection of Mn porphyrins has been reported. The HPLC/uv/vis method used for the *in vivo* determination of the anionic porphyrin, $Mn^{III}TBAP^{3-}$ (also known $Mn^{III}TCPP^{3-}$) is not sensitive enough [30,31]. We have previously developed a HPLC/uv/vis method for the separation of atropoisomers of cationic porphyrins, H_2Talkyl-2-PyP^{4+} and its Zn and Mn complexes, (alkyl being methyl, ethyl butyl and hexyl) from aqueous solutions [32]. Using ^{1}H NMR and X-ray we were able to identify the individual atropoisomers (αααα, αααβ, ααββ and αβαβ) separated by HPLC [32]. Yet, uv/vis detection is

not sensitive enough for the low *in vivo* levels of porphyrins. For this study we have developed a very sensitive HPLC/fluorescence method which is based on the exchange of the porphyrin Mn^{2+} site with Zn^{2+}, followed by the fluorescence detection of Zn^{II}TE-2-PyP^{4+}.

Experimental - General

Porphyrins

Mn^{III}TE-2-PyP^{5+} (454 nm, log ε = 5.14) [5], and ZnTE-2-PyP^{5+} (425.5nm, log ε=5.46) [33] were prepared as described previously.

Zn^{II}TnBu-2-PyP^{4+} was used as an internal standard and was prepared as was its ethyl analogue, ZnTE-2-PyP^{4+}. *Elemental analysis* for Zn^{II}TnBu-2-Py$PCl_4 \times 12.5\ H_2O$: Calculated: C, 52.65; H, 6.70; N, 8.77; Cl, 11.10. Found: C, 52.65; C; H, 6.07; N, 8.76; Cl, 11.21. The log values of m*olar absorptivities* of Zn^{II}TnBu-2-PyP^{5+}, were 4.46 (263.5 nm); 4.52 (327.0 nm), 5.64 (426.0 nm), 4.43 (557.0 nm) and 3.88 (593.5 nm).

Sodium L-ascorbate, mannitol, bovine serum albumin (BSA), sucrose and ethyleneglycol-bis (-aminoethylether)-*N*′, *N*, *N*′, *N*′-tetraacetic acid (EGTA) and $ZnSO_4 \times 7\ H_2O$ were from Sigma and $Zn(CH_3COO)_2 \times 2\ H_2O$ from J. T. Baker. Acetonitrile and trifluoroacetic acid (TFA) were from Fisher Scientific and triethylamine from Pierce. Methanol (anhydrous, absolute) was from Mallinckrodt. Glacial acetic acid was from EM Science. Phosphate-buffered saline (50 mM Na phosphate, 0.9% NaCl, pH 7.4) (PBS) was from Gibco. Anti-MnSOD was from Upstate, Lake Placid, NY, anti-Lamin A from Santa Cruz, CA, and anti-β-actin from Sigma, St. Louis, MO.

Uv/vis spectroscopy

Uv/vis was done on a Shimadzu 2501 PC UV/Vis spectrophotometer.

HPLC—Equipment: Waters 2695 HPLC system (pump, autosampler, column oven) and a Waters, model 2475 fluorescence detector set on Gain 100, λ_{exc} =425 nm and λ_{abs} = 656 nm [34–36]. Column: YMC-Pack, ODS-AM, C18 column (3 μm particle size, 120 A pore size, 150 × 4.6 mm) at 45°C. Elution gradient at 1.5 mL/min: 0–15–20 min, 100% A - 80% A - 100% A, followed by 5 min column conditioning. Solvent A: 95% aqueous (deionized water, 20 mM triethylamine, pH 2.7 adjusted with concentrated TFA) and 5% acetonitrile. Solvent B: acetonitrile. Autosampler temperature: 4°C. Injection volume: 80 μL.

Methods

Transformation of the Mn^{III}TE-2-PyP^{5+} into its fluorescent form

Mn(III) porphyrins are non-fluorescent [37]. Yet when the Mn^{3+} is replaced by a redox inactive metal, such as zinc, the metalloporphyrin becomes fluorescent [33]. This fact was used as a basis in the development of a highly sensitive method for the detection of minute quantities of MnTE-2-PyP^{5+} in the mice heart mitochondria homogenates.

Optimization of the Mn^{2+} to Zn^{2+} metal exchange

The Mn^{III}TE-2-PyP^{5+} is a stable complex, and even in 98% sulfuric acid no observable loss of Mn occured within 24 hours [16]. However, the reduced Mn(II) porphyrin is a labile complex, and in the presence of excess zinc a metal exchange occurs leading to the formation of Zn^{II} TE-2-PyP^{4+} (Scheme I). The pH most favorable for this exchange was 6.2. Lower pH causes the protonation of ascorbic acid (pK_a = 4.04 [38]), and thus slows the reduction of Mn^{3+} to Mn^{2+}. It also causes the demetallation of the Zn porphyrin [39]. Higher pH causes the precipitation of Zn hydroxo species (pK_a=10.6 for the $Zn^{II}(H_2O)_2^{2+} \Rightarrow Zn^{II}(H_2O)(OH)^+ +$

H^+) [40]. Therefore, the fastest exchange and best chromatography were obtained in acetonitrile-free HPLC solvent A whose acidity was adjusted with diluted trifluoroacetic acid to pH 6.2. The exchange was significantly faster with Zn acetate than with Zn sulfate. Briefly, the 6 μM Mn^{III}TE-2-PyP^{5+} was reduced aerobically by 8.3 mM ascorbate to Mn^{II}TE-2-PyP^{4+} in acetonitrile-free solvent A, pH 6.2, as followed by the Soret band shift from 454 nm to 438 nm [41]. Subsequently, 0.16 M Zn acetate was added and the metal exchange was followed on a Shimadzu 2501 PC UV/Vis spectrophotometer as the disappearance of Mn^{II}TE-2-PyP^{4+} Soret band at 438 nm, and appearance of 425.5 nm Zn^{II}TE-2-PyP^{4+} Soret band [33] (Figure 1). The exchange was completed within either 14 hours at 25°C or 1 hr at 50°C.

Mn^{III}TE-2-PyP^{5+}- treatment/heart mitochondria isolation

The University of Kentucky Medical Center Research Animal Facility has a continuously accredited program from AAALAC International. All experiments using animals were performed according to the approved protocol for humane care and use of animals. Eleven C57BL/6 mice were used for the study. Three animals were injected with saline only. Eight mice were injected intraperitoneally with 10 mg/kg of MnTE-2-PyP^{5+} in saline. This dose was chosen based on a number of *in vivo* experiments where this and similar doses were used [21,22,25,26]. The mice weighted from 20 to 25 g; thus the volumes of porphyrin solution or saline injected ranged accordingly from 200 to 250 μL. Two animals were euthanatized with high-dose pentobarbital at 4 hours, and another nine animals at 7 hours after the injection of either porphyrin or saline. Before harvesting tissue, the animals were perfused with saline to avoid artifacts related to the retention of blood in the heart.

Heart mitochondria was isolated as described previously by Mela and Seitz [42,43]. Briefly, the hearts were collected, rinsed in ice-cold isolation buffer (0.225 M manitol, 0.075 M sucrose, 1 mM EGTA, pH 7.4), and cut into small pieces. The heart tissue was washed three times with the isolation buffer to remove any residual blood, and was homogenized at 500 rpm with a chilled Teflon pestle in a glass cylinder with ten strokes. The homogenate was centrifuged at 480×g at 4°C for 5 min in a Sorval SS 34 rotor. The resulting supernatant was filtered through a double-layered cheesecloth, and was centrifuged at 7700×g at 4°C for 10 min. Supernatant was saved to check for leakage from mitochondria using MnSOD, a mitochondrial matrix enzyme, as an indicator by Western blotting. The pellet was rinsed with 0.5 mL of the isolation buffer with gentle shaking to remove the “fluffy layer” (damaged mitochondria) on top of the pellet. The wall of the centrifuge tube was cleaned with cotton swabs to remove lipids. The pellet was washed by gentle re-suspension in 3 mL isolation buffer using the smooth surface of a glass rod, and centrifuged at 7700×g at 4°C for 10 min. The supernatant was saved to again check for leakage from the mitochondria. The washing was repeated once more. The resulting mitochondria were collected for further analysis. The purity of mitochondria was examined using Lamin A (a nuclear protein) and β-actin (a cytoskeletal protein) as indicators by Western blotting and is shown in Figure 2. The protein levels were determined by colorimetric assay (Bio-Rad, Richmond, CA).

Mn^{III}TE-2-PyP^{5+} extraction/analysis

Heart mitochondrial homogenate (100 μL) was transferred into a 2 mL polypropylene screw-cap vial. Then, 200 μL of deionized water and 300 μL of 1% acetic acid in methanol were added and mixed by vortexing for 30 sec. After incubation for 30 min and again vortexing for 30 s, the homogenate was centrifuged 5 min at 16,000 g to separate proteins. The 400 μL of the supernatant was pipetted into a 5 mL polypropylene tube (10 × 50 mm). Solvent was completely removed in a Savant Speed-Vac evaporator at 40°C within 1 h. The dry residue was dissolved in a 100 μL of deionized water containing 20 mM triethylamine, the acidity of which was adjusted with diluted TFA to pH 6.2, followed by two cycles of 30 sec vortexing

and centrifugation for 2 min at 2000 g. 80 μL of the supernatant was transferred into a 2 mL polypropylene screw-cap tube, and 30 μL of 1.0 M Zn acetate in water and 10 μL of freshly prepared 0.11 M sodium ascorbate in water were added. The solution was left either overnight at 25°C or for one hour at 50°C. Then 20 μL of 2.7 M TFA and 20 μL of 100 nM Zn^{II}TnBu-2-PyP^{4+} were added, followed by vortexing for 30 sec and centrifugation for 5 min at 16,000 g. The supernatant (110 μL) was transferred to an HPLC autosampler polypropylene vial equipped with a silicone/PTFE septum.

All four atropoisomers of Zn^{II}TE-2-PyP^{5+} were present in the chromatogram at the abundance ratio reported previously [32] (Figure 3). Zn^{II}TnBu-2-PyP^{4+} was used as an internal standard, and its atropisomers were also present in the chromatogram at the expected abundance ratio (Figure 3) [32]. The assignment of the individual atropoisomers, αααα, αααβ, ααββ and αβαβ, of both Zn porphyrins was done based on our previous HPLC/^{1}H NMR/X-ray study [32].

Calibration curve

A set of serially diluted standard samples of Mn^{III}TE-2-PyP^{5+} from 1.25 ng/mL to100 ng/mL in either mitochondrial homogenate that had 3 mg protein/mL (Figure 4), or in 3 mg BSA/mL PBS (Figure 4, inset) was used to construct the calibration curve. With BSA/PBS the internal standard, ZnTnBu-2-PyP^{4+} was added at 375 nM concentration, while with mitochondrial homogenate 10-fold less ZnTnBu-2-PyP^{4+} (37.5 nM) was used, giving rise to a 10-fold difference in response. Response was calculated as the ratio between standard peak area/ internal standard peak area.

We compared curves obtained when using either αααβ isomer (most abundant) peak area or total area under peaks of all 4 isomers and obtained identical slopes. However, by using only αααβ peak our lowest limit of quantification (LLD) is better because quantification of the least abundant αβαβ isomer at those concentration values is not possible (LLD would be limited by the area of the least abundant isomer). In our experience [32] we do not see changes in atropo-isomer abundance distribution after administration/extraction of the compound to/from animals.

Recovery of MnTE-2-PyP^{5+} (the overall efficacy of extraction from mitochondria plus Mn to Zn exchange) was 98 %, and was determined in the following way. A known amount of MnTE-2-PyP^{5+} was added to mitochondrial homogenate (3mg/mL protein), and the procedure of extraction/metal exchange was followed. The response from this experiment was compared to the response of the sample where corresponding amount of ZnTE-2-PyP^{4+} (equal to 100% yield of MnTE-2-PyP^{5+}) was diluted into mobile phase.

Results and Discussion

Mitochondria are thought to be the major source of intracellular reactive species under normal and several pathological conditions. Thus injury to mitochondria contributes to a number of human pathologies. Not surprisingly, therapeutics targeting mitochondria have been intensively sought.

Mn^{III}TE-2-PyP^{5+} and its mode of action/s

Based on structure-activity relationships between the catalytic rate constant for $O_2^{\cdot-}$ dismutation and the $E_{1/2}$ for the $M^{III}P/M^{II}P$ redox couple [5], we have developed several potent catalytic Mn porphyrin-based antioxidants, Mn^{III}TE-2-PyP^{5+} being the best characterized. We have shown that Mn^{III}TE-2-PyP^{5+} is remarkably effective both *in vitro* [5–18] and *in vivo* [19–29] as a consequence of its several readily accessible oxidation states (+2, +3, +4 and +5)

[5,15,17]. It catalytically dismutes superoxide with log k_{cat} of 7.76 [5], whereas the log k_{cat} for SOD enzyme is between 9.3 and 8.84 [44–49]. Due to the ready reducibility of Mn^{III}TE-2-PyP^{5+}, the elimination of superoxide is likely coupled to the reduction of Mn^{III}TE-2-PyP^{5+} with cellular reductants [15,17]. Radi's group studied the peroxynitrite-related chemistry of Mn^{III}TE-2-PyP^{5+} showing that it is among the fastest reductants for peroxynitrite and for carbonate radical [10,14,15]. The elimination of peroxynitrite is coupled to the reduction of both Mn^{III}TE-2-PyP^{5+} and O=Mn^{IV}TE-2-PyP^{4+} by cellular reductants [15]. Given the rapid reaction between nitric oxide and superoxide ($k = 2 \times 10^{10}\ M^{-1}s^{-1}$) [50], it is highly likely that elimination of peroxynitrite may be the predominant mode of action of Mn^{III}TE-2-PyP^{5+} [14,15,51].

Since the observation that μM Mn^{III}TE-2-PyP^{5+} fully protects SOD-deficient *Escherichia coli* against aerobic inhibition of growth [5,19], the compound has been successfully used in *in vivo* studies where oxidative stress is a putative factor [20–28). The most remarkable data were obtained on cancer [20,21], radioprotection [25], and diabetes [22,26,52,53]. Recent data suggest that Mn^{III}TE-2-PyP^{5+} affects signaling pathways through inactivation of transcription factors such as AP-1 [20], HIF-1 [21], and NF-κB [29,52,53]. Two different mechanisms seem to be involved. The first relates to the ability of Mn^{III}TE-2-PyP^{5+} to redox-modulate signaling pathways through decreasing levels or reactive oxygen and nitrogen species involved in the activation of transcription factors [20,21]. The second mechanism relates to the inhibition of NF-κB, by oxidation of exposed cysteine thiol groups on its p50 subunit upon translocation into the nucleus [52,53]. Based on the results of Ferrer-Sueta et al O=Mn^{IV}TE-2-PyP^{4+}, formed from the oxidation of Mn^{III}TE-2-PyP^{5+} by peroxynitrite (or less efficiently by H_2O_2), can in turn rapidly oxidize glutathione [15,17] and thus presumably protein cysteines as well. It is likely that both mechanisms may occur in parallel.

Recently, Ferrer-Sueta *et al* have shown, with submitochondrial particles, that ≥ 3 μM Mn^{III}TE-2-PyP^{5+} protects peroxynitrite, superoxide, or carbonate radical-sensitive targets in mitochondria, while utilizing complexes I and II of mitochondrial electron transport with NADH or succinate as substrates [14]. This study is intended to complement their research by showing that despite significant hydrophilicity as a result of its high positive charge, which is essential for its antioxidant potency, Mn^{III}TE-2-PyP^{5+} is indeed able to get into the mouse heart mitochondria, following a single intraperitoneal administration, and at levels high enough to protect mitochondrial respiration from oxidative damage.

In vivo detection of Mn^{III}TE-2-PyP^{5+}

Despite the efficacy of MnTE-2-PyP^{5+} in a number of animal studies, a sensitive method for its *in vivo* determination has been lacking. Studies, indicating the inhibition of transcription factors [20,21,29,52], the mimicking of MnSOD [20], and the oxidation of p50 subunit of NF-κB [52], imply that Mn^{III}TE-2-PyP^{5+} distributes within the cell interior, and presumably into organelles as well. For the purpose of this work we have developed a new and sensitive method based on the reduction of Mn^{III}TE-2-PyP^{5+} by ascorbate, followed by the exchange of Mn^{2+} with Zn^{2+}, followed by HPLC/fluorescence detection of Zn^{II}TE-2-PyP^{4+} (Scheme I, Figure 1). Given the high fluorescence of Zn^{II}TE-2-PyP^{4+}, we were able to detect porphyrin levels as low as 0.5 ng/mg of protein. Calibration curves obtained by either diluting MnTE-2-PyP^{5+} into mitochondrial homogenate (Figure 4), or into BSA/PBS (Figure 4, inset) were linear in the range from 1.25 (+/− 3%) to 100 (+/− 1%) ng/mL of homogenate. There was a 10-fold difference in otherwise essentially identical slopes due to the 10-fold difference in the amount of internal standard used (0.00186 with BSA/PBS and 0.0191 with mitochondrial homogenate) (Figure 4). Thus BSA/PBS can be used instead of mitochondrial homogenate as a valid and more convenient alternative calibration medium for Mn porphyrin determination.

The *ortho* isomers of Mn^{III}TE-2-PyP^{5+}, Zn^{II}TE-2-PyP^{4+} and their parent metal-free ligand, H_2TE-2-PyP^{4+} have atropoisomers, which we have previously characterized by HPLC/uv/vis/NMR and X-ray methods [32]. We observed that the abundance ratio of four isomers of Zn^{II}TE-2-PyP^{4+} and their retention times on HPLC were the same in processed heart homogenates or in aqueous solution [32], indicating the absence of strong interactions of any of the four atropoisomers with cellular components (Figure 3 and ref 32). Our data also imply that the Mn porphyrin does not undergo oxidative degradation or any other modification *in vivo*. The method is suitable for the analysis of a variety of biological samples [54]. It may further be useful for the studies of other cationic Mn(III) porphyrins that we have been developing [8]. We are currently suing the method for the ongoing pharmacokinetic study of MnTE-2-PyP^{5+} in mice.

Mn^{III}TE-2-PyP^{5+} levels in mitochondria

Our data show that Mn^{III}TE-2-PyP^{5+} localizes in mouse heart mitochondria after a single 10 mg/kg intraperitoneal dose. The (2.95 ± 0.56) ng/mg protein of Mn^{III}TE-2-PyP^{5+} were found (Table 1). The same levels were obtained at 4 or 7 hours after the administration. The mitochondrial volume reported elsewhere varied greatly from essentially being non-existent [55,56] to as much as 1.2 μL/mg protein [55–62]. (The upper limit of 1.2 μL/mg protein was previously utilized by Radi *et al* [63] and Quijano *et al* [64] to calculate concentrations of mitochondrial MnSOD and cytochrome *c* to be 20 μM and 400 μM, respectively). Based on an average value of mitochondrial volume of 0.6 μL/mg protein, the calculated Mn^{III}TE-2-PyP^{5+} concentration in mitochondria is 5.1 μM. Ferrer-Sueta et al have shown that MnTE-2-PyP^{5+} was able to divert peroxynitrite from inactivation of succinate dehydrogenase and succinate oxidase equally efficiently at 3 μM (81%), 5 μM (85%) or 10 μM (83%), but not at 1 μM (28%) [14]. Thus based on their data and our findings, the 5.1 μM concentration of MnTE-2-PyP^{5+}, achieved in mitochondria after single administration is high enough to protect mitochondrial respiration against peroxynitrite-mediated oxidative damage [5,10,14,15]. Additionally, at such levels MnTE-2-PyP^{5+} can compete for $ONOO^-$ with CO_2, and can additionally intercept a substantial amount of $CO_3^{\cdot -}$.

This work answers affirmatively an important question as to whether Mn^{III}TE-2-PyP^{5+} and similar, highly-charged metalloporphyrins are capable of entering mitochondrion at levels high enough to exert there their presumed antioxidant action. Moreover it indicates that having been taken into mitochondria *in vivo* the Mn porphyrin resists washing out during isolation of the mitochondria.

Conclusions

The new and sensitive method developed herein enables us to show that, despite its hydrophilicity, i.e. overall high positive charge, which is essential for its in vivo antioxidant efficacy, Mn^{III}TE-2-PyP^{5+} targets mitochondria after only single dose of 10 mg/kg, achieving micromolar levels that are sufficient to exert protection of the mitochondrial respiration from oxidative damage. Therefore, along with the report of Ferrer-Sueta et al [14] this study justifies further improvement of Mn(III) porphyrins as therapeutics for protecting mitochondria from oxidative damage.

Acknowledgements

Ivan Spasojeviæ acknowledges NIH/NCI Duke Comprehensive Cancer Center Core Grant (5-P30-CA14236-29). Ines Batini -Haberle appreciates financial support from NIH- IR21-ESO/3682, W19A167798-01, and NIH U19 AI67798-01. Yumin Chen, Marsha Cole, Yunfeng Zhao, Teresa Noel and Daret St. Clair are thankful to the support of NIH grants CA 49797, CA 73599 and CA 94853. Authors are also thankful to Rafael Radi and Gerardo Ferrer-Sueta for helpful discussions and to Irwin Fridovich for critical reading of the manuscript and for his continuous support.

References

1. James AM, Cocheme HM, Smith RAJ, Murphy MP. Interactions of mitochondria-targeted and untargeted ubiquinones with the mitochondrial respiratory chain and reactive oxygen species. J Biol Chem 2005;28:21295–21312. [PubMed: 15788391]
2. Smith RAJ, Porteous CM, Ganes AM, Murphy MP. Delivery of bioactive molecules to mitochondria. Proc Natl Acad Sci 2003;100:5407–5412. [PubMed: 12697897]
3. Dhanasekaran A, Kotamraju S, Karunakaran C, Kalivendi SV, Thomas S, Joseph J, Kalyanaraman JJB. Mitochondria superoxide dismutase mimetic inhibits peroxide-induced oxidative damage and apoptosis: Role of mitochondrial superoxide. Free Radic Biol Med 2005;39:567–583. [PubMed: 16085176]
4. Asayama S, Kawamura E, Nagaoka S, Kawakami H. Design of manganese porphyrin modified with mitochondrial signal peptide for a new antioxidant. Mol Pharm 2006;3:468–470. [PubMed: 16889441]
5. Batinic-Haberle I, Benov L, Spasojevic I, Hambright P, Crumbliss AL, Fridovich I. The Relationship Between Redox Potentials, Proton Dissociation Constants of Pyrrolic Nitrogen, and *in Vitro* and *in Vivo* Superoxide Dismutase Activities of Manganese(III) and Iron(III) Cationic and Anionic Porphyrins. Inorg Chem 1999;38:4011–4022.
6. Spasojevic I, Batinic-Haberle I. Manganese(III) Complexes with Porphyrins and Related Compounds as Scavengers of Superoxide. Inorg Chim Acta 2001;317:230–242.
7. Kachadourian R, Batinic-Haberle I, Fridovich I. Syntheses and SOD-like Activities of Partially Chlorinated Manganese(III)-5,10,15,20-Tetrakis(*N*-methylpyridinium-2-yl)Porphyrin. Inorg Chem 1999;38:391–396.
8. Batinic-Haberle I, Spasojevic I, Stevens RD, Bondurant B, Okado-Matsumoto A, Fridovich I, Vujaskovic Z, Dewhirst MW. New PEG-ylated Mn(III) porphyrins approaching catalytic activity of SOD enzyme. Dalton Trans 2006:617–624. [PubMed: 16402149]
9. Batinic-Haberle I, Spasojevic I, Stevens RD, Hambright P, Neta P, Okado-Matsumoto A, Fridovich I. New Class of Potent Catalysts of O_2^- Dismutation. Mn(III) methoxyethylpyridyl- and methoxyethylimidazolylporphyrins. J Chem Soc Dalton Trans 2004:1696–1702.
10. Ferrer-Sueta G, Vitturi D, Batinic-Haberle I, Fridovich I, Goldstein S, Czapski G, Radi R. Reactions of Manganese Porphyrins with Peroxynitrite and Carbonate Radical Anion. J Biol Chem 2003;278:27432–27438. [PubMed: 12700236]
11. Spasojevic I, Batinic-Haberle I, Reboucas JS, Idemori YM, Fridovich I. Electrostatic Contribution in the Catalysis of O_2^- Dismutation by Superoxide Dismutase Mimics. J Biol Chem 2003;278:6831–6837. [PubMed: 12475974]
12. Batinic-Haberle I, Spasojevic I, Stevens RD, Hambright P, Fridovich I. Manganese(III) *Meso* Tetrakis *Ortho N*-alkylpyridylporphyrins. Synthesis, Characterization and Catalysis of O_2^- Dismutation. J Chem Soc Dalton Trans 2002:2689–2696.
13. Batinic-Haberle I. Manganese Porphyrins and Related Compounds as Mimics of Superoxide Dismutase. Methods Enzymol 2001;349:223–233. [PubMed: 11912911]
14. Ferrer-Sueta G, Hanninbal L, Batinic-Haberle I, Radi R. Reduction of manganese porphyrins by flavoenzymes and submitochondrial particles: A catalytic cycle for the reduction of peroxynitrite. Free Radic Biol Med 2006;41:503–512. [PubMed: 16843831]
15. Ferrer-Sueta G, Batinic-Haberle I, Spasojevic I, Fridovich I. Peroxynitrite Scavanging by Manganese (III) Meso-Tetrakis-(*N*-methylpyridyl)Porphyrins. Chem Res Toxicol 1999;12:442–449. [PubMed: 10328755]
16. Batinic-Haberle I, Benov L, Spasojevic I, Fridovich I. The *Ortho* Effect Makes Manganese (III) *Meso*-Tetrakis(*N*-methylpyridinium-2-yl)Porphyrin (MnTM-2-PyP) a Powerful and Potentially Useful Superoxide Dismutase Mimic. J Biol Chem 1998;273:24521–24528. [PubMed: 9733746]
17. Batinic-Haberle I, Spasojevic I, Fridovich I. Tetrahydrobiopterin Rapidly Reduces SOD Mimic, Mn (III) tetrakis(N-ethylpyridinium-2-yl)porphyrin. Free Radic Biol Med 2004;37:367–374. [PubMed: 15223070]
18. Day BJ, Batinic-Haberle I, Crapo JD. Metalloporphyrins are Potent Inhibitors of Lipid Peroxidation. Free Rad Biol Med 1999;26:730–736. [PubMed: 10218663]

19. Okado-Matsumoto A, Batinic-Haberle I, Fridovich I. Complementation of SOD deficient *Escherichia coli* by manganese porphyrin mimics of superoxide dismutase. Free Radic Biol Med 2004;37:401–410. [PubMed: 15223074]
20. Zhao Y, Chaiswing L, Oberley TD, Batinic-Haberle I, StClair W, Epstein CJ, StClair D. A mechanism-based antioxidant approach for the reduction of skin carcinogenesis. Cancer Res 2005;65:1401–1405. [PubMed: 15735027]
21. Moeller BJ, Batinic-Haberle I, Spasojevic I, Rabbani ZN, Anscher MS, Vujaskovic Z, Dewhirst MW. Effects of a catalytic metalloporphyrin antioxidant on tumor radioresponsiveness. Int J Rad Oncol Biol Phys 2005;63:545–552.
22. Benov L, Batinic-Haberle I. A manganese porphyrin SOD mimic suppresses oxidative stress and extends the life span of streptozotocin-diabetic rats. Free Radic Res 2005;38:81–88. [PubMed: 15875815]
23. Sheng H, Spasojevic I, Warner DS, Batinic-Haberle I. Mouse spinal cord compression injury is ameliorated by intrathecal manganese(III) porphyrin. Neurosci Lett 2004;366:220–225. [PubMed: 15276251]
24. Sheng H, Enghild J, Bowler R, Patel M, Calvi CL, Batinic-Haberle I, Day BJ, Pearlstein RD, Crapo JD, Warner DS. Effects of Metalloporphyrin Catalytic Antioxidants in Experimental Brain Ischemia. Free Radic Biol Med 2002;33:947–961. [PubMed: 12361805]
25. Vujaskovic Z, Batinic-Haberle I, Rabbani ZN, Feng Q-F, Kang SK, Spasojevic I, Samulski TV, Fridovich I, Dewhirst MW, Anscher MS. A Small Molecular Weight Catalytic Metalloporphyrin Antioxidant with Superoxide Dismutase (SOD) Mimetic Properties Protects Lungs from Radiation-Induced Injury. Free Radic Biol Med 2002;33:857–863. [PubMed: 12208373]
26. Piganelli JD, Flores SC, Cruz C, Koepp J, Young R, Bradley B, Kachadourian R, Batinic-Haberle I, Haskins K. A Metalloporphyrin Superoxide Dismutase Mimetic (SOD Mimetic) Inhibits Autoimune Diabetes. Diabetes 2002;51:347–355. [PubMed: 11812741]
27. Mackensen GB, Patel M, Sheng H, Calvi CL, Batinic-Haberle I, Day BJ, Liang LP, Fridovich I, Crapo JD, Pearlstein RD, Warner DS. Neuroprotection from Delayed Post-Ischemic Administration of a Metalloporphyrin Catalytic Antioxidant in the Rat. J Neurosci 2001;21:4582–4592. [PubMed: 11425886]
28. Aslan M, Ryan TM, Adler B, Townes TM, Parks DA, Thompson JA, Tousson A, Gladwin MT, Tarpey MM, Patel RP, Batinic-Haberle I, White CR, Freeman BA. Oxygen Radical Inhibition of Nitric-Oxide Dependent Vascular Function in Sickle Cell Disease. Proc Natl Acad Sci USA 2001;98:15215–15220. [PubMed: 11752464]
29. Bottino R, Balamurugan AN, Bertera S, Pietropaolo M, Trucco M, Piganelli JD. Preservation of human islet cell functional mass by anti-oxidative action of a novel SOD mimic compound. Diabetes 2002;51:2561–2567. [PubMed: 12145171]
30. Li Q-Y, Pedersen C, Day BJ, Patel M. Dependence of excitotoxicity neurodegeneration on mitochondrial aconitase inactivation. J Neurochem 2001;78:746–755. [PubMed: 11520895]
31. Oury TD, Thakker K, Menache M, Chang L-Y, Crapo JD, Day BJ. Attenuation of bleomycin-induced pulmonary fibrosis by a catalytic antioxidant metalloporphyrin. Am J Resp Cell Mol Biol 2001;25:164–169.
32. Spasojevic I, Menzeleev R, White PS, Fridovich I. Rotational Isomers of *N*-alkylpyridylporphyrins and their Metal Complexes. HPLC Separation, ^{1}H NMR and X-ray Structural Characterization, Electrochemistry and Catalysis of O_2^- Disproportionation. Inorg Chem 2002;41:5874–5881. [PubMed: 12401096]
33. Benov L, Batinic-Haberle I, Spasojevic I, Fridovich I. Isomeric *N*-alkylpyridylporphyrins and their Zn(II) Complexes: Inactive as SOD Mimics but are Powerful Photosenzitizers. Arch Biochem Biophys 2002;402:159–165. [PubMed: 12051659]
34. Kalyanasundaram K. Photochemistry of water-soluble porphyrins: Comparative study of isomeric tetrapyridyl- and tetrakis(N-methylpyridiniumyl)porphyrins. Inorg Chem 1984;23:2453–2459.
35. Vergeldt FJ, Koehorst RBM, Van Hoek A, Schaafsma TJ. Intramolecular interactions in the ground and excited state of tetrakis(N-methylpyridyl)porphyrins. J Phys Chem 1995;99:4397–4405.
36. Quimby DJ, Longo FR. Luminescence studies of several tetrarylporphyrins and their Zn derivatives. J Am Chem Soc 1975;97:5111–5117.

37. Harriman A, Porter G. Photochemistry of manganese porphyrins. Part 4.- Photosensitized reductions of quinines. J Chem Soc Farady II 1980;76:1429–1441.
38. Taqui Khan MM, Martell AE. The kinetics of reaction of iron(III) chelates of aminopolycarboxylic acids with ascorbic acid. J Am Chem Soc 1968;90:3386–3389. [PubMed: 5651561]
39. Hambright P, Batinic-Haberle I, Spasojevic I. Meso Tetrakis Ortho, Meta and Para *N*-alkylpyridylporphyrins: Kinetics of Copper(II) and Zinc(II) Incorporation and Zinc Porphyrin Demetalation. J Porphyrins Phthalocyanines 2003;7:139–146.
40. Kragten, J. Atlas of metal-ligand equilibria in aqueous solution. Halstead Press; New York: 1978.
41. Spasojevic I, Batinic-Haberle I, Fridovich I. Nitrosylation of Manganese(II) Tetrakis(*N*-ethylpyridinium-2-yl)Porphyrin. Nitric Oxide: Biology and Chemistry 2000;4:526–533.
42. Mela L, Seitz S. Isolation of mitochondria with emphasis on heart mitochondria from small amounts of tissue. Methods Enzymol 1979;55:39–46. [PubMed: 459851]
43. Nedergaard J, Cannon B. Overview-preparation and properties of mitochondria from different sources. Methods Enzymol 1979;55:3–28. [PubMed: 459848]
44. Lawrence GD, Sawyer DT. Potentiometric titrations and oxidation-reduction potentials of manganese and copper-zinc superoxide dismutases. Biochemistry 1979;18:3045–3050. [PubMed: 380641]
45. Barrette WC Jr, Sawyer DT, Free JA, Asada K. Potentiometric titrations and oxidation-reduction potentials of several iron superoxide dismutases. Biochemistry 1983;22:624–627. [PubMed: 6340720]
46. Ellerby RM, Cabelli DE, Graden JA, Valentine JS. Copper-Zinc Superoxide Dismutase: Why Not pH-Dependent? J Am Chem Soc 1996;118:6556–6561.
47. Vance CK, Miller AF. A Simple Proposal That Can Explain the Inactivity of Metal-Substituted Superoxide Dismutases. J Am Chem Soc 1998;120:461–467.
48. Michel E, Nauser T, Sutter B, Bounds PL, Koppenol WH. Arch Biochem Biophys 2005;439:234–240. [PubMed: 15978540]
49. Goldstein S, Fridovich I, Czapski G. Kinetic properties of Cu,Zn-superoxide dismutase as a function of metal content –Order restored. Free Radic Biol Med 2006;41:937–941. [PubMed: 16934676]
50. Nauser T, Koppenol WH. The rate constant of the reaction of superoxide and nitrogen monoxide: approaching the diffusion limit. J Phys Chem A 2002;106:4084–4086.
51. Ferrer-Sueta G, Quijano C, Alvarez B, Radi R. Reactions of manganese porphyrins and manganese-superoxide dismutase with peroxynitrite. Methods Enzymol 2002;349:23–3. [PubMed: 11912912]
52. Tse H, Milton MJ, Piganelli JD. Mechanistic analysis of the immunomodulatory effects of a catalytic antioxidant on antigen-presenting cells: Implication for their use in targeting oxidation/reduction reactions in innate immunity. Free Radic Biol Med 2004;36:233–247. [PubMed: 14744635]
53. Bottino R, Balamurugan AN, Tse H, Thirunavukkarasu C, Ge X, Profozich J, Milton M, Ziegenfuss A, Trucco M, Piganelli JD. Response of human islets to isolation stress and the effect of antioxidant treatment. Diabetes 2004;53:2559–2568. [PubMed: 15448084]
54. Spasojevic I, Batinic-Haberle I, Yumin C, Noel T, Lichun Z, StClair DK. MnTE-2-PyP^{5+} pharmacokinetics. In preparation
55. Nedergaard J, Cannon B. Apparent masking of [^{3}H]GDP binding in rat brown-fat mitochondria is due to mitochondrial swelling. Eur J Biochem 1987;164:681–686. [PubMed: 3569283]
56. Cohen NS, Cheung C-W, Raijman L. Measurements of mitochondrial volumes are affected by the amount of mitochondria used in determinations. Biochem J 1987;245:375–379. [PubMed: 2444215]
57. Halestrap AP, Quinlan PT. The intramitochondrial volume measured using sucrose as an extramitochondrial marker overestimates the true matrix volume determined with manitol. Biochem J 1983;214:387–393. [PubMed: 6412699]
58. Halestrap AP, Dunlop JL. Intramitochondrial regulation of fatty acid b-oxidation occurs between flavoprotein and ubiquinone. Biochem J 1986;239:559–565. [PubMed: 3827814]
59. Beavis AD, Brannan RD, Garlid KD. Swelling and contraction of mitochondrila matrix. I. A structural interpretation of the relationship between light scattering and matrix volume. J Biol Chem 1985;260:13424–13433. [PubMed: 4055741]
60. Radi R, Turrens JF, Freeman BA. Cytochrome *c*-catalyzed membrane lipid peroxidation by hydrogen peroxide. Arch Biochem Biophys 1991;288:118–125. [PubMed: 1654818]

61. Halestrap AP, Quinlan PT, Whipps DE, Armston AE. Regualtion of the mitochondrial matrix volume *in vivo* and *in vitro*. The role of calcium. Biochem J 1986;236:779–787. [PubMed: 2431681]

62. Rickwood, D.; Wilson, MT.; Darley-Usmar, VM. Mitochondria. IRL Press; Oxford: 1987.

63. Radi R, Turrnes JF, Freeman BA. Cytochrome c-catalyzed membrane lipid peroxidation by hydrogen peroxide. Arch Biochem Biophys 1991;288:118–125. [PubMed: 1654818]

64. Quijano C, Hernandez-Saavedra D, Castro L, McCord JM, Freeman BA, Radi R. Reaction of peroxynitrite with Mn-superoxide dismutase. Role of the metal center in decomposition kinetics and nitration. J Biol Chem 2001;276:11631–11638. [PubMed: 11152462]

Abbreviations

SOD
: superoxide dismutase

NHE
: normal hydrogen electrode

MnP
: any Mn(III) porphyrin

***para* isomer**
: Mn^{III}TM-4-PyP^{5+}, Mn(III) *meso*-tetrakis(*N*-methylpyridinium-4-yl)porphyrin

***ortho* isomer**
: Mn^{III}TE-2-PyP^{5+}, Mn(III) *meso*-tetrakis(*N*-ethylpyridinium-2-yl)porphyrin (AEOL-10113)

Mn^{III}TBAP^{3-}(also known as MnTCPP^{3-})
: Mn(III) *meso*-tetrakis(4-carboxylatophenyl)porphyrin

Zn^{II}TE-2-PyP^{4+}
: Zn *meso*-tetrakis(*N*-ethylpyridinium-2-yl)porphyrin

Zn^{II}TnBu-2-PyP^{4+}
: Zn *meso*-tetrakis(*N*-n-butylpyridinium-2-yl)porphyrin

H_2Talkyl-2-PyP^{4+}*meso*-tetrakis(*N*-alkylpyridinium-2-yl)porphyrin
: alkyl being methyl (M), ethyl (E), n-butyl (nBu) and n-hexyl (nHex)

meso
: is indicating substitution in 5,10,15,20 positions on porphyrin core

HIF-1
: hypoxia inducible factor-1,

NF-κB
: nuclear factor -κB

AP-1
: activator protein-1

BSA
: bovine serum albumine

TFA
: trifluoroacetic acid

PBS

phosphate-buffered saline

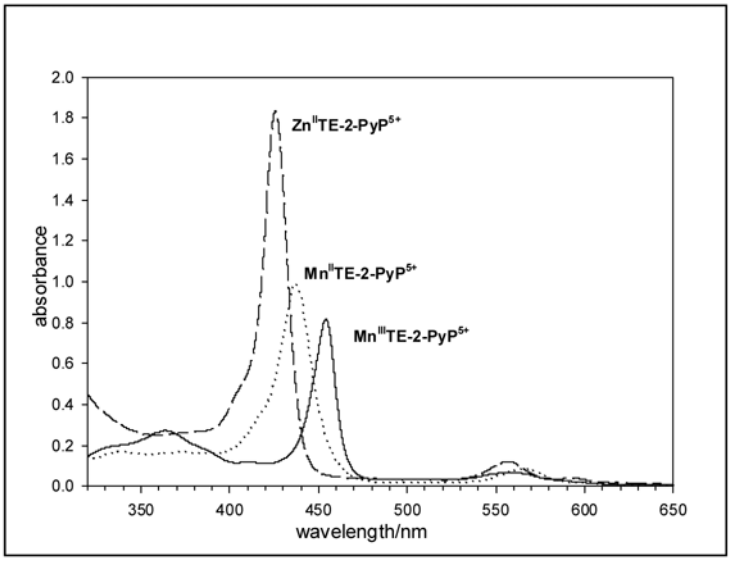

Figure 1.

The spectral change associated with $Mn^{III}P$ reduction, followed by Zn^{2+} for Mn^{2+} exchange at 6 μM total porphyrin concentration, 8.3 mM ascorbic acid, and 0.16 M Zn acetate in acetonitrile-free HPLC solvent A, pH 6.2, 25°C.

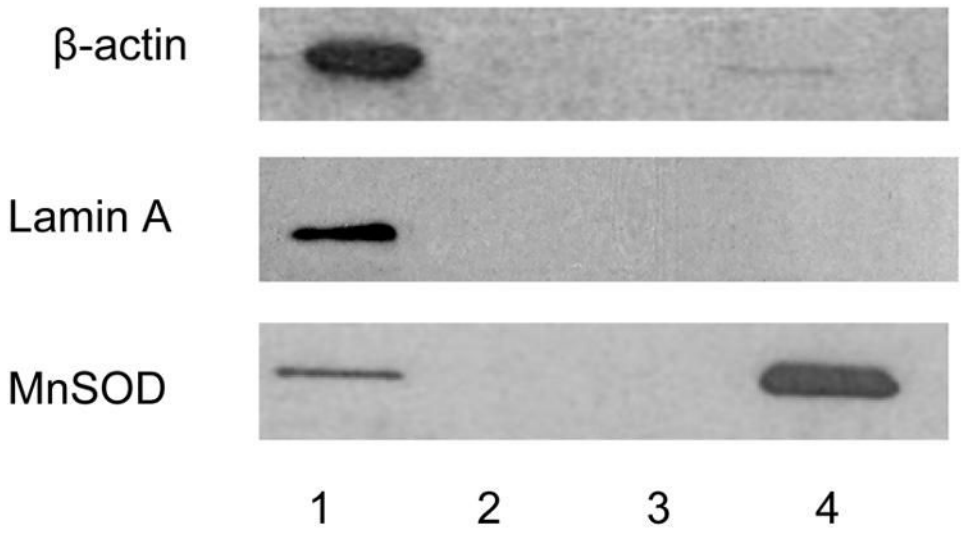

Figure 2.

Integrity and purity of isolated mitochondria. Mitochondria were purified by centrifuging heart homogenate on a mannitol-sucrose gradient twice. Western blot probing for Lamin A (a nuclear protein) and β-actin (a cytoskeletal protein) indicated minimum contamination from non-mitochondrial fractions, and Western blot probing against MnSOD indicated there was no leaking of the purified mitochondria. **Lane 1**. Supernatant from centrifugation of whole heart homogenate; **Lane 2**. Supernatant from first washing; **Lane 3**. Supernatant from second washing; **Lane 4**. Purified mitochondria.

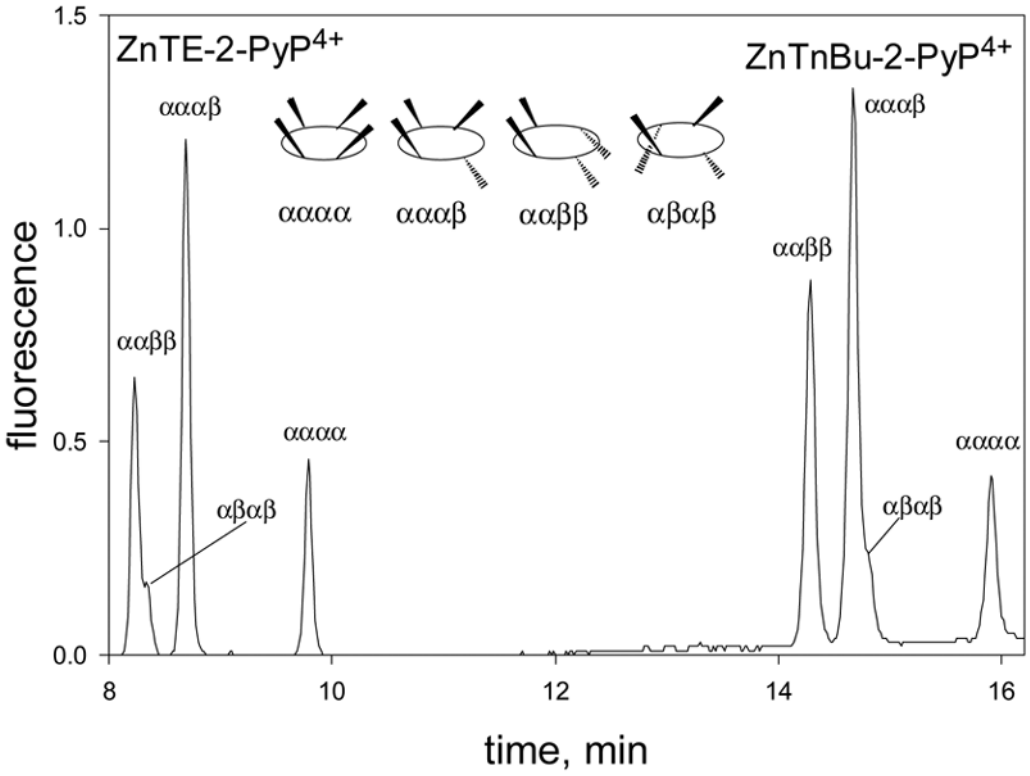

Figure 3.

The representative HPLC chromatogram of 33.3 nM Zn^{II}TE-2-PyP^{4+}. The 37.5 nM Zn^{II}TnBu-2-PyP^{4+} was the internal standard. The individual atropoisomers were assigned based on our previous HPLC/^{1}H NMR/X-ray study [32]. The "α"denotes an *N*-alkyl above the porphyrin plane, and "β" below the plane [32].

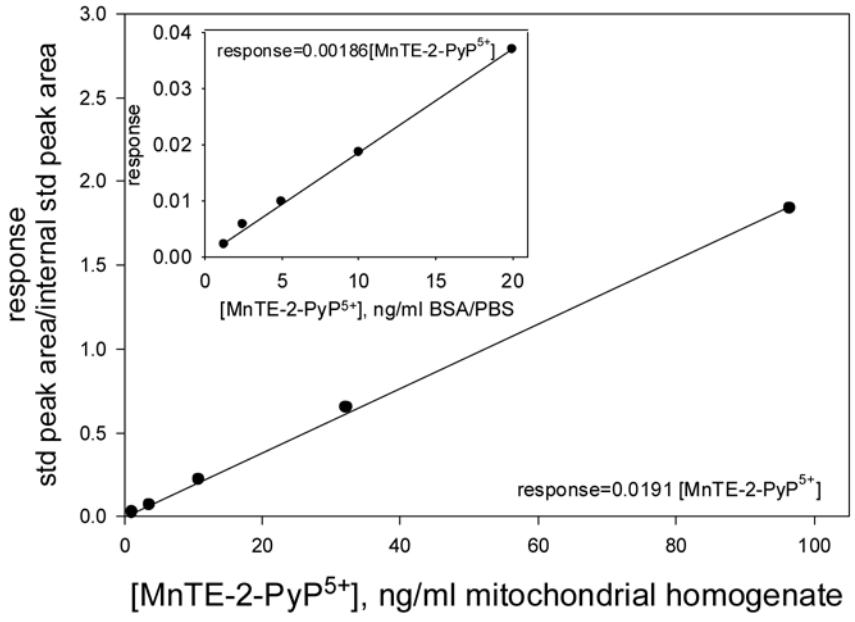

Figure 4.

Calibration curves for the determination of MnTE-2-PyP^{5+} levels *in vivo*. The curves were prepared by diluting MnTE-2-PyP^{5+} into either mitochondrial homogenate or into BSA/PBS (inset) whose protein concentration was 3mg/mL homogenate. With BSA/PBS the internal standard was added at 375 nM concentration, while with mitochondrial homogenate 10-fold less ZnTnBu-2-PyP^{4+} (37.5 nM) was used. Thus there is a 10-fold difference in otherwise identical slopes (0.00186 and 0.0191). BSA/PBS can be therefore used instead of mitochondrial homogenate, as a less costly alternative calibration medium for determination of Mn porphyrin levels *in vivo*.

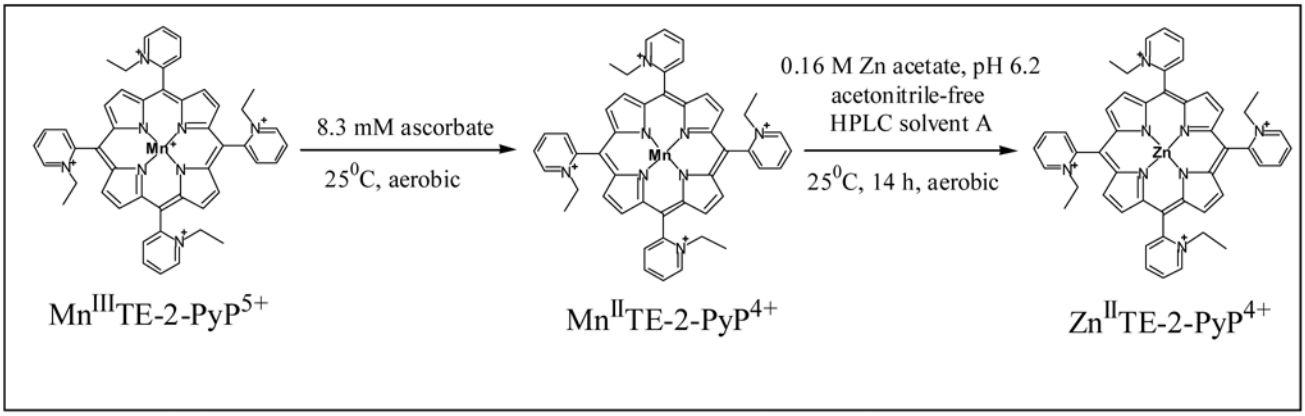

Scheme I.

The exchange of porphyrin Mn^{2+} with Zn^{2+}, under conditions shown below, was used as a basis for the HPLC/fluorometric method for the determination of MnTE-2-PyP^{5+} levels *in vivo*.

Table 1

The levels of Mn^{III}TE-2-PyP^{5+} in C57BL/6 mouse heart mitochondria. The mean value was calculated to be (2.95 ± 0.56) ng/mg protein.

Mouse	drug10 mg/kg i.p.	total protein mg/mL homogenate	Mn^{III}TE-2-PyP^{5+} ng/mL homogenate	Mn^{III}TE-2-PyP^{5+} ng/mg protein
Mice were sacrificed 7 hours after drug administration				
1	Mn^{III}TE-2-PyP^{5+}	2.820	6.55	2.32
2	Mn^{III}TE-2-PyP^{5+}	2.543	6.75	2.65
3	Mn^{III}TE-2-PyP^{5+}	2.682	7.82	2.91
4	Mn^{III}TE-2-PyP^{5+}	2.833	8.15	2.88
5	Mn^{III}TE-2-PyP^{5+}	1.794	3.83	2.13
6	Mn^{III}TE-2-PyP^{5+}	1.824	7.17	3.93
Mice were sacrificed 4 hours after drug administration				
7	Mn^{III}TE-2-PyP^{5+}	1.223	4.28	3.50
8	Mn^{III}TE-2-PyP^{5+}	1.909	6.29	3.29
Control mice				
9	saline	3.147	0.00	0.00
10	saline	3.193	0.00	0.00
11	saline	2.940	0.00	0.00